



# Modeling and Sensitivity Analysis of Thermal Conductivity of Ethylene Glycol-Water Based Nanofluids with Alumina Nanoparticles

M.M. Rashidi<sup>1,2,3</sup> · M. Alhuyi Nazari<sup>4</sup> · I. Mahariq<sup>5</sup> · N. Ali<sup>5</sup>

Received: 2 January 2022 / Accepted: 1 March 2022 / Published online: 16 March 2022  
© The Society for Experimental Mechanics, Inc 2022, corrected publication 2022

## Abstract

Nanofluids containing alumina nanoparticles have been used in different thermal devices due to their favorable characteristics including ease of synthesis, relatively high stability and proper thermal features. Nanofluids thermal conductivity could be modeled with high exactness by employing intelligent techniques. In the current paper, thermal conductivity of EG-Water-based nanofluids with alumina particles is modeled by utilizing Multi-Layer Perceptron (MLP) and Group Method of Data Handling (GMDH) as two efficient intelligent approaches. In case of utilizing MLP two transfer functions, tangent sigmoid and radial basis functions, are applied. Results showed that utilizing MLP with radial basis provides the highest precision of the prediction in its optimal architecture.  $R^2$  of the models by applying MLP with tansig and radial basis functions and GMDH are 0.9998, 0.9998 and 0.9996, respectively. Furthermore, sensitivity analysis reveals that base fluid thermal conductivity has the most significant role in the thermal conductivity of the considered nanofluids.

**Keywords** Nanofluid · Thermal Conductivity · Sensitivity Analysis · Artificial Neural Network · Intelligent Method

## Introduction

Nanofluids, the fluids containing particles in nanometer dimensions, outperform common heat transfer liquids in thermal devices due to improved characteristics which is due to the dispersion of solid particles with higher Thermal Conductivity (TC) compared with the liquids. TC of the nanofluids is influenced by the features of fluid and nano-material, temperature, volume fraction etc. Improvement in the properties of the nanofluids, compared with pure liquids, makes them attractive for several applications [1, 2]. Heat transfer of nanofluid-filled cavity has been analyzed in different works by considering different factors [3–5]. As an example [6], nanofluid-filled cavity mixed convection in case of two-sided elastic walled and internal heat generation was investigated in a wok. It was concluded that mean Nusselt number increases with increment in the Volume Fraction (VF) solid phase. In another research [7], nanofluid mixed convection in shallow cavity was analyzed by utilizing two-phase mixture model. It was found that increment in the VF of solid phase causes enhancement in the convective heat transfer coefficient. Ebrahimi et al. [8] found enhancement in mixed convection heat transfer in a cavity with elbow shape by making use of Cu/water nanofluid.

---

✉ M.M. Rashidi  
mm\_rashidi@yahoo.com

M. Alhuyi Nazari  
Nazari.mohammad.a@ut.ac.ir

I. Mahariq  
Ibrahim.Maharik@aum.edu.kw

N. Ali  
Nawaf.ali@aum.edu.kw

<sup>1</sup> Institute of Fundamental and Frontier Sciences, University of Electronic Science and Technology of China, Chengdu 610054, Sichuan, People's Republic of China

<sup>2</sup> Mathematics and Applied Mathematics, University of Johannesburg, Johannesburg, South Africa

<sup>3</sup> Faculty of Mechanical and Industrial Engineering, Quchan University of Technology, Quchan, Iran

<sup>4</sup> Faculty of New Sciences and Technologies, University of Tehran, Tehran, Iran

<sup>5</sup> College of Engineering and Technology, American University of the Middle East, Egaila 54200, Kuwait



Metal oxide particles such as aluminum oxide (alumina), copper oxide, titanium dioxide (titania) are widely utilized in nanofluids regarding the simplicity of their synthesis and relatively high stability in different base fluids. The nanofluids containing metal oxide particles are usable in various thermal mediums and are able to remarkably improve the performance [9] which is mostly due to the modification of the TC. Aside the single liquid, the base fluids of the nanofluids could be composed of two or more liquids. Nanofluids with binary base fluids, consisting two liquids, have attracted attentions in recent years due to some of advantages such as wider applicability range. Nanofluids with mixture of Ethylene Glycol (EG) and water as the base fluid are convenient for various applications like car radiator [10], solar systems [11, 12] and thermal management units of energy technologies [13].

Nanofluids containing alumina are attractive for different thermal applications and able to drastically enhance heat transfer. For instance, Ghanbapour et al. [14] made use of  $\text{Al}_2\text{O}_3$ /water nanofluid in a screen mesh heat pipe and noted improvement in thermal performance for condition of dispersion of the nanomaterials in the operating fluid. Qu et al., [15] examined  $\text{Al}_2\text{O}_3$ /water nanofluid in an oscillation heat pipe and noticed around 32% reduction in the highest thermal resistance compared with water-filled one. Yousefi et al. [16] used  $\text{Al}_2\text{O}_3$ /water nanofluid in a solar collector and reached around 28% enhancement in the efficiency in case of 0.2% wt concentration. Tong et al. [17] used the nanofluid in a solar collector and compared the exergy efficiency with water as operating fluid. They noticed that exergy efficiency could be enhanced by approximately 57%. Bondarenko et al. [18] analyzed natural convection cavity with heat generating unit and observed that cooling process could be intensified by utilization of  $\text{Al}_2\text{O}_3$ /water nanofluid. Chamkha et al. [19] investigated single and double-lid cavities mixed convection with square shape and found that presence of  $\text{Al}_2\text{O}_3$  nanoparticles causes significant augmentation in heat transfer. Hashim et al. [20] investigated heat transfer in a wavy cavity and found that it increases compared with water by introducing  $\text{Al}_2\text{O}_3$ /water nanofluid.

Regarding the significance of TC in heat transfer characteristics of fluids, huge number of works have focused on this feature of nanofluid [21, 22]. Studies have shown that temperature, VF, specifications of fluid and nanomaterials mostly affect the TC [23]. Different models have been proposed for modeling of TC based on the obtained data from experimental works. According to the literature review, intelligence approaches have shown significant performance in exact prediction of TC. For instance, Maleki et al. [24] applied Multi-Layer Perceptron (MLP) and Group Method of Data Handling (GMDH) to model TC of nanofluids with ZnO as solid phase and found the  $R^2$  of the models was around 0.99. Ghazvini et al. [25]

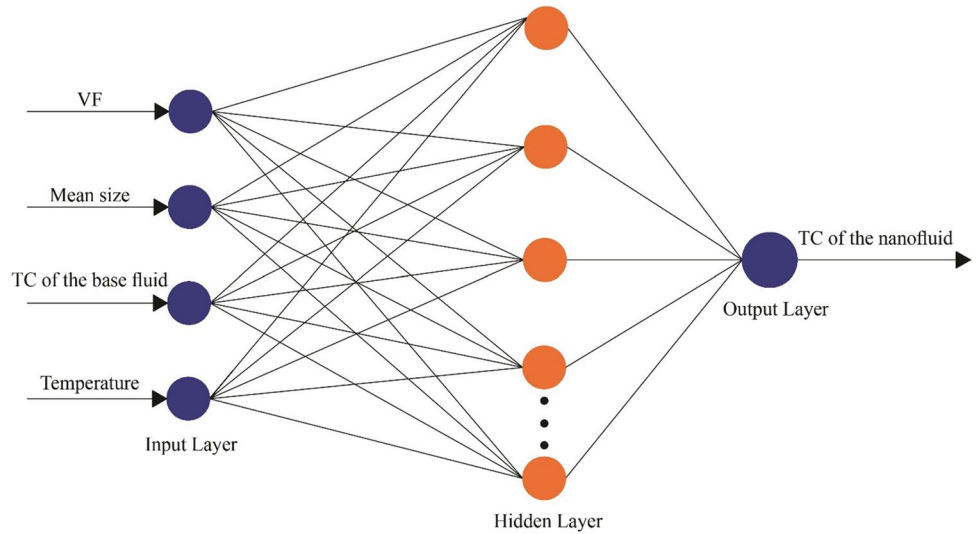
applied ANN to model TC of nanofluids with magnetic copper nanoparticles and water as the base fluid.  $R^2$  of their model was 0.99 that demonstrated the high precision of the predicted data. Pare et al. [21] used ANN to model TC of metal oxide/water nanofluids and noted good consistency of the predicted values with the experimental data. Esfe et al. [26] compared performance of Response Surface Methodology (RSM) and ANN in predicting TC of  $\text{TiO}_2$ /water and found that the correlation based on ANN outperform the one based on RSM.

Regarding the outstanding performance of ANNs in predicting the TC of nanofluids, this paper focuses on the utilizing of these methods for TC modeling of nanofluids containing alumina nanoparticles with EG-water base fluids in different mixture ratios. Till now, some studies have concentrated on the modeling of nanofluids with alumina particles; however, in these studies just a single base fluid such as water or EG are considered [27, 28], while the present works considers the nanofluids consisting of water-EG base fluid with different mixture ratios. Furthermore, sensitivity analysis is another factor that makes the current work more comprehensive compared with the similar works. In addition, in the previous studies, the methods are compared while the present study compares the performance of the models with two functions, in MLP with different architectures, and GMDH as another approach. The findings of the current work would provide the most appropriate approach and structure for modeling the nanofluids. Moreover, by applying the sensitivity analysis, degree of importance of each input variable will be clear and deeper insight into the influential factors would be obtained. Details of the study are presented in the upcoming sections.

## Methodology

ANNs are applicable for proposing regression model for various systems. Methods based on ANNs are used in large extent for predicting the properties of nanofluids. In current paper, two algorithms including MLP and GMDH are employed. MLP network is composed of three main layers. The input layer refers to the input variables used for proposing regression model; subsequently, Hidden Layer (HL) is applied for processing the data and providing the output and finally the output layer provides the predicted values. For cases of modeling complex problems, more than one HL can be used. The main processors of the networks are neurons. Schematic of a simple MLP is shown in Fig. 1. In this figure, vector of  $X$  is the network's inputs. By considering  $j$  as the numbers of neurons used in the network,  $w_{ji}$  is the weight of each neuron and  $y_j$  and  $u_j$  are network output and output linear combination which are defined as follows [29]:

Fig. 1 Schematic of MLP



$$u_j = \sum_{i=1}^n w_{ji} X_i \tag{1}$$

$$y_j = \varphi(u_j + b_j) \tag{2}$$

$$v_j = u_j + b_j \tag{3}$$

In the above equations,  $b_j$  is the tendency of the function and  $\varphi(0)$  denotes the activation function [29]. For assessing the effect of activation function, two conventional types including tangent sigmoid (tansig) and Radial Basis Function (RBF) are used here.

Another approach that is used here is GMDH. The processors of this network work on the basis of polynomials. The number of HLs in this network relies on the needed exactness. In the process of modeling with this network in case of single output with  $n$  inputs, Kolmogorov-Gabor polynomial is applied in the following form [30]:

$$P = \alpha_0 + \sum_{i=1}^n \omega_i X_i + \sum_{i=1}^n \sum_{j=1}^n \omega_{ij} X_i X_j + \sum_{i=1}^n \sum_{j=1}^n \sum_{k=1}^n \omega_{ijk} X_i X_j X_k + \dots \tag{4}$$

where  $w$  refers to the vector of weights and  $P$  is the predicted value. To determine the coefficients of the abovementioned equation, regression techniques are applied. These coefficients are calculated by considering the least value of Mean Squared Error (MSE) (Figs. 2 and 3).

In order to compare the models and evaluate their exactness, different criteria are used including MSE,  $R^2$  and Average Absolute Relative Deviation (AARD) that are determined as follows [31]:

$$MSE = \frac{\sum_{i=1}^n (y_i^{actual\ value} - y_i^{predicted\ value})^2}{n} \tag{5}$$

$$R^2 = 1 - \frac{\sum_{i=1}^{i=n} (y_i^{actual\ value} - y_i^{predicted\ value})^2}{\sum_{i=1}^{i=n} (y_i^{actual\ value} - \overline{y^{actual\ value}})^2} \tag{6}$$

$$AARD = \frac{\sum_{i=1}^n |y_i^{actual\ value} - y_i^{predicted\ value}|}{n} \tag{7}$$

where  $n$  refers to the number of samples.

## Results and Discussion

To propose a model, two references are used that were experimental works on the measurement of TC of nanofluids with different mixture ratios of EG and water as base fluids that are extracted from Refs [32, 33]. All of the nanofluids contained alumina particles in different VFs. The inputs employed for regression are base fluid TC at 20°C (W/m.K), VF (%), temperature (°C) and average size of particles (nm), which are represented in Table 1. It should be mentioned that the mixture ratios of the base fluid for water/EG were 40%/60%, 60%/40%, 80%/20% and 50%/50%. In case of MLP, the datasets were randomly split into training (70%), test (15%) and validation (15%) sets while for GMDH just training (70%) and test (30%) are applied. As mentioned, two types of

**Fig. 2** Modeled data vs measured values for MLP with tansig

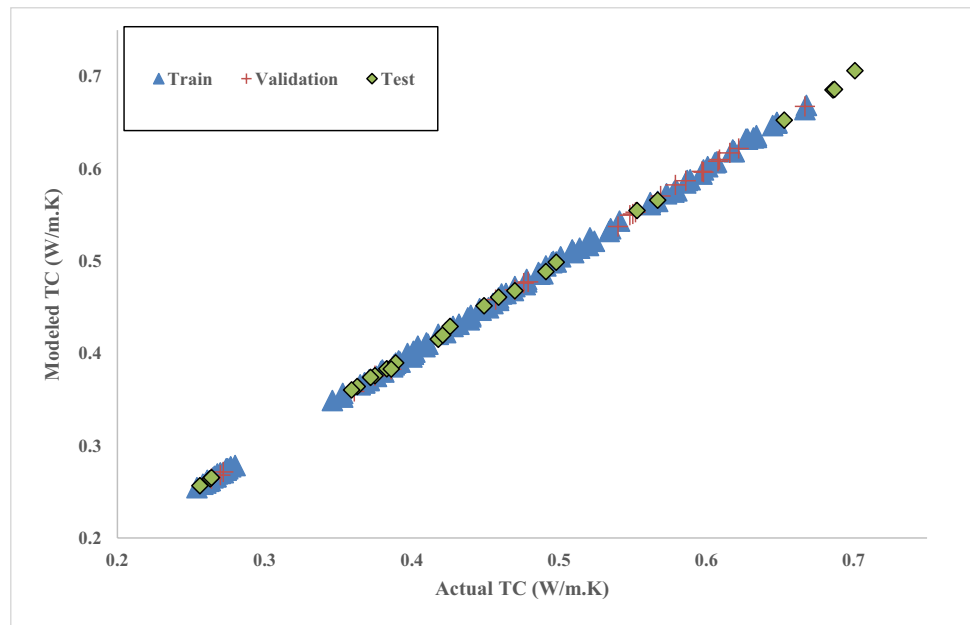


**Fig. 3** Modeled data vs measured values for MLP with RBF

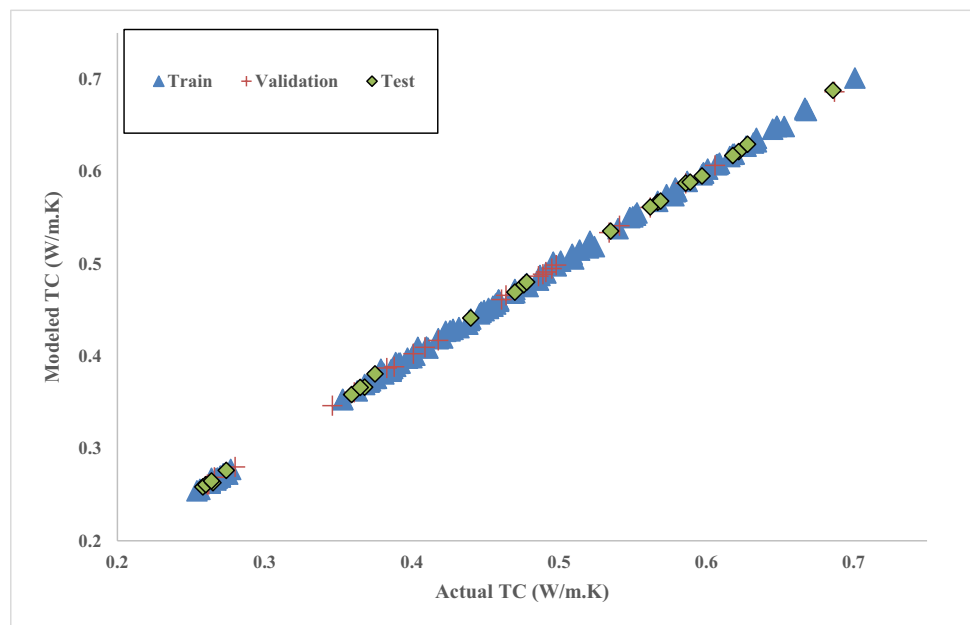


**Table 1** Ranges of input variables

Variables	Ranges
TC of base fluids at 20°C (W/m.K)	0.253–0.492
VF (%)	0.2–1.5
Temperature (°C)	10–60
Average size of particles (nm)	13–36

activation functions are used for MLP. In Table 1, MSE of the networks with various numbers of neurons and tansig function are represented. On the basis of overall data MSE, utilization of 13 neurons in the HL causes the highest exactness with MSE of  $3.43 \times 10^{-6}$ . In this case,  $R^2$  is 0.9998 which demonstrates significant exactness of the applied model in prediction. Closer values of  $R^2$  to 1 means higher exactness of the regression and this obtained value for the present model indicates acceptable accuracy of the prediction. In Table 2, obtained values by the model are evaluated based on their consistency with

**Table 2** MSE of different architectures in case of using tansig

Number of Neurons	MSE Values			
	Training	Validation	Test	Overall
4	$1.147 \times 10^{-5}$	$1.229 \times 10^{-5}$	$1.329 \times 10^{-5}$	$1.187 \times 10^{-5}$
5	$8.39 \times 10^{-6}$	$4.97 \times 10^{-6}$	$1.18 \times 10^{-5}$	$8.38 \times 10^{-6}$
6	$4.41 \times 10^{-6}$	$6.82 \times 10^{-6}$	$4.16 \times 10^{-6}$	$4.73 \times 10^{-6}$
7	$7.4 \times 10^{-6}$	$7.17 \times 10^{-6}$	$6.61 \times 10^{-6}$	$7.25 \times 10^{-6}$
8	$3.8 \times 10^{-6}$	$2.43 \times 10^{-6}$	$5.88 \times 10^{-6}$	$3.91 \times 10^{-6}$
9	$4.55 \times 10^{-6}$	$2.42 \times 10^{-6}$	$6.92 \times 10^{-6}$	$4.58 \times 10^{-6}$
10	$7.48 \times 10^{-6}$	$5.06 \times 10^{-6}$	$1.25 \times 10^{-5}$	$7.88 \times 10^{-6}$
11	$3.23 \times 10^{-6}$	$4.09 \times 10^{-6}$	$1.86 \times 10^{-5}$	$5.66 \times 10^{-6}$
12	$5.51 \times 10^{-6}$	$6.33 \times 10^{-6}$	$5.09 \times 10^{-6}$	$5.57 \times 10^{-6}$
13	$3.58 \times 10^{-6}$	$2.34 \times 10^{-6}$	$3.82 \times 10^{-6}$	$3.43 \times 10^{-6}$
14	$3.78 \times 10^{-6}$	$3.76 \times 10^{-6}$	$4.99 \times 10^{-6}$	$3.96 \times 10^{-6}$
15	$4.59 \times 10^{-6}$	$3.79 \times 10^{-6}$	$4.81 \times 10^{-6}$	$4.50 \times 10^{-6}$

**Table 3** MSE of different architectures in case of using RBF

Number of Neurons	MSE Values			
	Training	Validation	Test	Overall
4	$1.421 \times 10^{-5}$	$1.263 \times 10^{-5}$	$1.342 \times 10^{-5}$	$1.385 \times 10^{-5}$
5	$6.48 \times 10^{-6}$	$1.08 \times 10^{-5}$	$8.4 \times 10^{-6}$	$7.41 \times 10^{-6}$
6	$9.38 \times 10^{-6}$	$5.69 \times 10^{-6}$	$1.06 \times 10^{-5}$	$9.01 \times 10^{-6}$
7	$6.93 \times 10^{-6}$	$1.08 \times 10^{-5}$	$6.69 \times 10^{-6}$	$7.48 \times 10^{-6}$
8	$7.37 \times 10^{-6}$	$1.22 \times 10^{-5}$	$7.81 \times 10^{-6}$	$8.16 \times 10^{-6}$
9	$3.87 \times 10^{-6}$	$3.8 \times 10^{-6}$	$4.62 \times 10^{-6}$	$3.97 \times 10^{-6}$
10	$5.12 \times 10^{-6}$	$4.59 \times 10^{-6}$	$3.71 \times 10^{-6}$	$4.83 \times 10^{-6}$
11	$7.76 \times 10^{-6}$	$1.37 \times 10^{-5}$	$7.1 \times 10^{-6}$	$8.54 \times 10^{-6}$
12	$4.41 \times 10^{-6}$	$5.8 \times 10^{-6}$	$4.24 \times 10^{-5}$	$4.59 \times 10^{-6}$
13	$3.8 \times 10^{-6}$	$1.48 \times 10^{-6}$	$2.89 \times 10^{-6}$	$3.32 \times 10^{-6}$
14	$4.02 \times 10^{-6}$	$2.35 \times 10^{-6}$	$2.05 \times 10^{-6}$	$3.48 \times 10^{-6}$
15	$3.51 \times 10^{-6}$	$3.46 \times 10^{-6}$	$8.66 \times 10^{-6}$	$4.28 \times 10^{-6}$

the corresponding measured data. Lower values of MSE, which means closer to 0, demonstrate closer predicted data to the actual ones and higher exactness. On the basis of these values, for all of the numbers of neurons applied in the networks, the MSE values are acceptable; however, the network with 13 neurons led to lower MSE compared with other architectures.

Similar to the network with tansig function, different neurons are applied for the case of RBF. In Table 3, MSE of the model for different neuron numbers are shown. According to the values, applying 13 neurons in the HL leads to the lowest MSE which is around  $3.32 \times 10^{-6}$  and lower than the corresponding value for the case of employing tansig function in the network. In this case, MSE is very low and close to 0 which denotes the significant exactness of the proposed models. In this condition,  $R^2$  is

0.9998, very close to 1, which shows the closeness of the predicted and measured values.

In the next stage, TC was predicted by making use of GMDH by applying GMDH Shell Software. In Fig. 4, modeled and measured data by use of this method are depicted. In this case, MSE of train, test and overall data are  $5.102 \times 10^{-6}$ ,  $9.33 \times 10^{-6}$  and  $6.370 \times 10^{-6}$ , respectively. Compared with optimal MLP networks, MSE is higher in this case that means lower precision of this model. In this condition,  $R^2$  is equal to 0.9996, which is lower in comparison with the previous models; however, its accuracy is acceptable and the predicted data are close to the corresponding actual ones. Finally, in this section of paper, the models are compared on the basis of AARD. For the MLP with tansig and RBF, and GMDH, AARD are around 0.323%, 0.289% and 0.442%, respectively. Based on the determined values of these criteria, it can be concluded that MLP with RBF outperforms other two methods for modeling the TC of considered nanofluids.

### Sensitivity Analysis

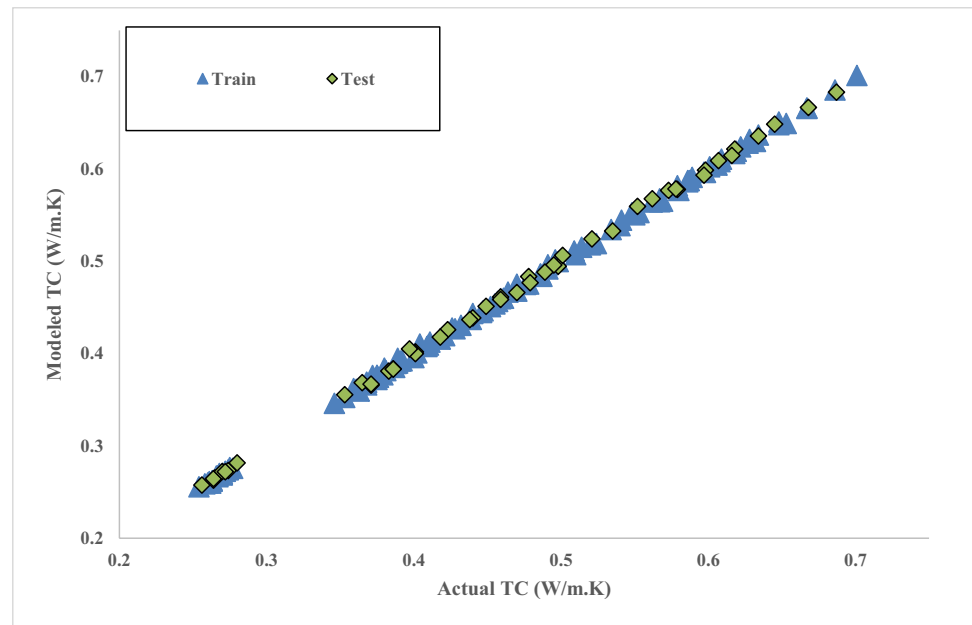
According to the experimental data, it can be concluded that increment in both temperature and VF of the considered nanofluids causes improvement in the TC. In addition, due to the high dependency of the TC of nanofluids on the base fluid characteristics, it is anticipated to have higher TC in cases of nanofluids with higher TC of base fluid. Data on the dependency of the TC on the particle size are in contradiction with each other in some studies [34]. To assess the output dependency on the variables applied as the inputs sensitivity analysis is applied. It is performed by considering relevancy factor that is between  $-1$  and  $1$ . Higher absolute relevancy factor means higher effect of the corresponding variable. Positive and negative signs of this factor refer to the fact that increment in the output is as a consequence of the input variable increase or reduction, respectively. Relevancy factor can be calculated by using Eq. (8) as follows [35]:

$$r = \frac{\sum_{i=1}^N (X_{k,i} - \bar{X}_k)(y_i - \bar{y})}{\sqrt{\sum_{i=1}^N (X_{k,i} - \bar{X}_k)^2 \sum_{i=1}^N (y_i - \bar{y})^2}} \tag{8}$$

In Eq. (5),  $y_i$  and  $\bar{y}$  are the  $i$ th output and mean value of output, respectively.  $X_{k,i}$  and  $\bar{X}_k$  are the  $i$ th value of the  $k$ th input and mean value of the  $k$ th input, respectively. On the basis of the abovementioned equation, the relevancy of the base fluid TC is the most significant input that is followed by particle size, temperature and VF, respectively. In order to get deeper insight into the dependency of the TC on the mentioned factors, it is suggested to consider more data from



**Fig. 4** Modeled data vs measured values for GMDH



different references in the future works. It should be mentioned that the results of this research can be helpful for nanofluid simulations [36, 37].

## Conclusion

The present article focused on the proposing of model for TC of nanofluids with water-EG base fluids in different mixture ratios that contain alumina nanoparticles by making use of MLP with tansig and RBF and GMDH. Results revealed that all of the proposed models are significantly accurate in modeling the TC; however, MLP with RBF was a little better.  $R^2$  of the models using the MLP with tansig and RBF and GMDH were 0.9998, 0.9998 and 0.9996, respectively. AARD of these models were around 0.323%, 0.289% and 0.442%, respectively. In addition, sensitivity analysis was conducted on the applied variables and it was observed that base fluid TC is the most influential among the considered variables on the value of nanofluid TC.

## Declarations

**Conflict of interests** There is no conflict of interests between the authors.

## References

- Jarray A, Mehrez Z, El Cafsi A (2019) Mixed convection Ag-MgO/water hybrid nanofluid flow in a porous horizontal channel. *The European Physical Journal Special Topics* 2019 228:12 228:2677–2693. <https://doi.org/10.1140/EPJST/E2019-900068-8>
- Hanif H, Khan I, Shafie S (2021) A novel study on hybrid model of radiative Cu–Fe<sub>3</sub>O<sub>4</sub>/water nanofluid over a cone with PHF/PWT. *The European Physical Journal Special Topics* 2021 230:5 230:1257–1271. <https://doi.org/10.1140/EPJS/S11734-021-00042-Y>
- Ahrar AJ, Djavareshkian MH (2016) Lattice Boltzmann simulation of a Cu-water nanofluid filled cavity in order to investigate the influence of volume fraction and magnetic field specifications on flow and heat transfer. *J Mol Liq* 215:328–338. <https://doi.org/10.1016/J.MOLLIQ.2015.11.044>
- Mansour MA, Armaghani T, Chamkha AJ, Rashad AM (2019) Entropy generation and nanofluid mixed convection in a C-shaped cavity with heat corner and inclined magnetic field. *The European Physical Journal Special Topics* 2019 228:12 228:2619–2645. <https://doi.org/10.1140/EPJST/E2019-900050-3>
- Moayed H (2021) Investigation of heat transfer enhancement of Cu-water nanofluid by different configurations of double rotating cylinders in a vented cavity with different inlet and outlet ports. *International Communications in Heat and Mass Transfer* 126:105432. <https://doi.org/10.1016/J.ICHEATMASSTRANSFER.2021.105432>
- Selimefendigil F, Öztop HF (2015) Mixed convection in a two-sided elastic walled and SiO<sub>2</sub> nanofluid filled cavity with internal heat generation: Effects of inner rotating cylinder and nanoparticle's shape. *J Mol Liq* 212:509–516. <https://doi.org/10.1016/J.MOLLIQ.2015.09.037>
- Goodarzi M, Safaei MR, Vafai K, Ahmadi G, Dahari M, Kazi SN, Jomhari N (2014) Investigation of nanofluid mixed convection in a shallow cavity using a two-phase mixture model. *Int J Therm Sci* 75:204–220. <https://doi.org/10.1016/J.IJTHERMALSCI.2013.08.003>
- Ebrahimi D, Yousefzadeh S, Akbari OA, Montazerifar F, Rozati SA, Nakhjavani S, Safaei MR (2021) Mixed convection heat transfer of a nanofluid in a closed elbow-shaped cavity (CESC). *Journal of Thermal Analysis and Calorimetry* 2021 144:6 144:2295–2316. <https://doi.org/10.1007/S10973-021-10548-1>



9. Alhuyi Nazari M, Ahmadi MH, Ghasempour R, Shafii MB (2018) How to improve the thermal performance of pulsating heat pipes: A review on working fluid. *Renew Sust Energ Rev* 91:630–638. <https://doi.org/10.1016/j.rser.2018.04.042>
10. Heris SZ, Shokrgozar M, Poorpharhang S, Shanbedi M, Noie SH (2014) Experimental Study of Heat Transfer of a Car Radiator with CuO/Ethylene Glycol-Water as a Coolant. *J Dispers Sci Technol* 35:677–684. <https://doi.org/10.1080/01932691.2013.805301>
11. Fikri MA, Asri FF, Faizal WM, Adli HK, Mamat R, Azmi WH, Najafi G, Yusaf T (2020) TiO<sub>2</sub>-SiO<sub>2</sub> nanofluid characterization: Towards efficient with water/ethylene glycol mixture for solar application. *IOP Conference Series: Materials Science and Engineering* 863:012055. <https://doi.org/10.1088/1757-899X/863/1/012055>
12. Menbari A, Alemrajabi AA, Ghayeb Y (2016) Experimental investigation of stability and extinction coefficient of Al<sub>2</sub>O<sub>3</sub>-CuO binary nanoparticles dispersed in ethylene glycol-water mixture for low-temperature direct absorption solar collectors. *Energy Convers Manag* 108:501–510. <https://doi.org/10.1016/J.ENCONMAN.2015.11.034>
13. Zakaria I, Mohamed WANW, Mamat AMIB, Saidur R, Azmi WH, Mamat R, Talib SFA (2015) Experimental Investigation of Al<sub>2</sub>O<sub>3</sub> - Water Ethylene Glycol Mixture Nanofluid Thermal Behaviour in a Single Cooling Plate for PEM Fuel Cell Application. *Energy Procedia* 79:252–258. <https://doi.org/10.1016/J.EGYPRO.2015.11.474>
14. Ghanbarpour M, Nikkam N, Khodabandeh R, Toprak MS, Muhammed M (2015) Thermal performance of screen mesh heat pipe with Al<sub>2</sub>O<sub>3</sub> nanofluid. *Exp Thermal Fluid Sci* 66:213–220. <https://doi.org/10.1016/J.EXPTHERMFLUSCI.2015.03.024>
15. Qu J, Wu H (2010) ying; Cheng, P. Thermal performance of an oscillating heat pipe with Al<sub>2</sub>O<sub>3</sub>-water nanofluids. *International Communications in Heat and Mass Transfer* 37:111–115. <https://doi.org/10.1016/j.icheatmasstransfer.2009.10.001>
16. Yousefi T, Veysi F, Shojaeizadeh E, Zinadini S (2012) An experimental investigation on the effect of Al<sub>2</sub>O<sub>3</sub>-H<sub>2</sub>O nanofluid on the efficiency of flat-plate solar collectors. *Renew Energy* 39:293–298. <https://doi.org/10.1016/J.RENENE.2011.08.056>
17. Tong Y, Lee H, Kang W, Cho H (2019) Energy and exergy comparison of a flat-plate solar collector using water, Al<sub>2</sub>O<sub>3</sub> nanofluid, and CuO nanofluid. *Appl Therm Eng* 159:113959. <https://doi.org/10.1016/J.APPLTHERMALENG.2019.113959>
18. Bondarenko DS, Sheremet MA, Oztop HF, Ali ME (2019) Natural convection of Al<sub>2</sub>O<sub>3</sub>/H<sub>2</sub>O nanofluid in a cavity with a heat-generating element. *Heatline visualization. Int J Heat Mass Transf* 130:564–574. <https://doi.org/10.1016/J.IJHEATMASSTRANSFER.2018.10.091>
19. Chamkha AJ, Abu-Nada E (2012) Mixed convection flow in single- and double-lid driven square cavities filled with water-Al<sub>2</sub>O<sub>3</sub> nanofluid: Effect of viscosity models. *European Journal of Mechanics - B/Fluids* 36:82–96. <https://doi.org/10.1016/J.EUROMECHFLU.2012.03.005>
20. Hashim I, Alsabery AI, Sheremet MA, Chamkha AJ (2019) Numerical investigation of natural convection of Al<sub>2</sub>O<sub>3</sub>-water nanofluid in a wavy cavity with conductive inner block using Buongiorno's two-phase model. *Adv Powder Technol* 30:399–414. <https://doi.org/10.1016/J.APT.2018.11.017>
21. Pare A, Ghosh SK (2021) A unique thermal conductivity model (ANN) for nanofluid based on experimental study. *Powder Technol* 377:429–438. <https://doi.org/10.1016/J.POWTEC.2020.09.011>
22. Maleki A, Haghghi A, Irandoost Shahrestani M, Abdelmalek Z (2020) Applying different types of artificial neural network for modeling thermal conductivity of nanofluids containing silica particles. *J Therm Anal Calorim*. <https://doi.org/10.1007/s10973-020-09541-x>
23. Rashidi, M.M.; Nazari, M.A.; Mahariq, I.; Assad, M.E.H.; Ali, M.E.; Almuzaqer, R.; Nuhait, A.; Murshid, N. Thermophysical Properties of Hybrid Nanofluids and the Proposed Models: An Updated Comprehensive Study. *Nanomaterials* 2021, Vol. 11, Page 3084 2021, 11, 3084, <https://doi.org/10.3390/NANO11113084>
24. Maleki, A.; Elahi, M.; Assad, M.E.H.; Alhuyi Nazari, M.; Safdari Shadloo, M.; Nabipour, N. Thermal conductivity modeling of nanofluids with ZnO particles by using approaches based on artificial neural network and MARS. *Journal of Thermal Analysis and Calorimetry* 2020, 1–12, <https://doi.org/10.1007/s10973-020-09373-9>
25. Ghazvini M, Maddah H, Peymanfar R, Ahmadi MH, Kumar R (2020) Experimental evaluation and artificial neural network modeling of thermal conductivity of water based nanofluid containing magnetic copper nanoparticles. *Physica A: Statistical Mechanics and its Applications* 124127. <https://doi.org/10.1016/j.physa.2019.124127>
26. Hemmat Esfe M, Motallebi SM, Bahraei M (2021) Employing response surface methodology and neural network to accurately model thermal conductivity of TiO<sub>2</sub>-water nanofluid using experimental data. *Chin J Phys* 70:14–25. <https://doi.org/10.1016/J.CJPH.2020.12.012>
27. Ahmadi MH, Ahmadi MA, Nazari MA, Mahian O, Ghasempour R (2019) A proposed model to predict thermal conductivity ratio of Al<sub>2</sub>O<sub>3</sub>/EG nanofluid by applying least squares support vector machine (LSSVM) and genetic algorithm as a connectionist approach. *J Therm Anal Calorim* 135:271–281. <https://doi.org/10.1007/s10973-018-7035-z>
28. Ahmadi MH, Alhuyi Nazari M, Ghasempour R, Madah H, Shafii MB, Ahmadi MA (2018) Thermal conductivity ratio prediction of Al<sub>2</sub>O<sub>3</sub>/water nanofluid by applying connectionist methods. *Colloids Surf A Physicochem Eng Asp* 541:154–164. <https://doi.org/10.1016/J.COLSURFA.2018.01.030>
29. Khosrojerdi S, Vakili M, Yahyaei M, Kalhor K (2016) Thermal conductivity modeling of graphene nanoplatelets/deionized water nanofluid by MLP neural network and theoretical modeling using experimental results. *International Communications in Heat and Mass Transfer* 74:11–17. <https://doi.org/10.1016/J.ICHEATMASSTRANSFER.2016.03.010>
30. Wang N, Maleki A, Alhuyi Nazari M, Tlili I, Safdari Shadloo M (2020) Thermal conductivity modeling of nanofluids contain MgO particles by employing different approaches. *Symmetry* 12:206
31. Maleki A, Haghghi A, Mahariq I (2021) Machine learning-based approaches for modeling thermophysical properties of hybrid nanofluids: A comprehensive review. *J Mol Liq* 322:114843
32. Syam Sundar L, Venkata Ramana E, Singh MK, Sousa ACM (2014) Thermal conductivity and viscosity of stabilized ethylene glycol and water mixture Al<sub>2</sub>O<sub>3</sub> nanofluids for heat transfer applications: An experimental study. *International Communications in Heat and Mass Transfer* 56:86–95. <https://doi.org/10.1016/J.ICHEATMASSTRANSFER.2014.06.009>
33. Elias MM, Mahbulul IM, Saidur R, Sohel MR, Shahrul IM, Khaleduzzaman SS, Sadeghipour S (2014) Experimental investigation on the thermo-physical properties of Al<sub>2</sub>O<sub>3</sub> nanoparticles suspended in car radiator coolant. *International Communications in Heat and Mass Transfer* 54:48–53. <https://doi.org/10.1016/j.icheatmasstransfer.2014.03.005>
34. Özerinç, S.; Kakaç, S.; Yazıcıoğlu, A.G. Enhanced thermal conductivity of nanofluids: a state-of-the-art review. *Microfluidics and Nanofluidics* 2009 8:2 2009, 8, 145–170, <https://doi.org/10.1007/S10404-009-0524-4>
35. Baghban A, Kahani M, Nazari MA, Ahmadi MH, Yan W-M (2019) Sensitivity analysis and application of machine learning



- methods to predict the heat transfer performance of CNT/water nanofluid flows through coils. *Int J Heat Mass Transf* 128:825–835. <https://doi.org/10.1016/J.IJHEATMASSTRANSFER.2018.09.041>
36. Alagumalai A, Qin C, Vimal K, Solomine E, Yang L, Zhang P, Otanicar T, Kasaean A, Chamkha AJ, Rashidi MM, Wongwises S, Seon Ahn H, Lei Z, Saboori T, Mahian O (2022) Conceptual analysis framework development to understand barriers of nanofluid commercialization. *Nano Energy* 92:106736. <https://doi.org/10.1016/j.nanoen.2021.106736>
37. Rashidi MM, Sadri M, Sheremet M (2021) Numerical simulation of hybrid nanofluid mixed convection in a lid-driven square cavity with magnetic field using high order compact scheme. *Nanomaterials* 11(9):2250. <https://doi.org/10.3390/nano11092250>

**Publisher's Note** Springer Nature remains neutral with regard to jurisdictional claims in published maps and institutional affiliations.

